Role of Neurotoxin Associated Proteins in the Low pH Induced Structural Changes in the Botulinum Neurotoxin Complex

Gowri Chellappan[*], **Raj Kumar**[†], **Shuowei Cai**[*], and **Bal Ram Singh**[*,†,1]

[*]Department of Chemistry and Biochemistry, University of Massachusetts Dartmouth, North Dartmouth, MA 02747

[†]Botulinum Research Center, Institute of Advanced Sciences, Dartmouth, MA 02747

Abstract

BoNT (Botulinum Neurotoxin) produced by the bacterium *Clostridium botulinum* as a complex with NAPs causes botulism. It has been known that the NAPs protect the toxin from both extremes of pHs and proteases of the GI tract. In an attempt to emulate the physiological conditions encountered by the toxin, we examined BoNT/A, BoNT/A complex, and NAPs under different pH conditions and monitored their structural characteristics by far-UV CD and thermal denaturation analysis. BoNT/A complex showed the maximum CD signal with a molar ellipticity of -1.8×10^5 deg.cm^2/dmol at 222 nm at both acidic and neutral pHs. Thermal denaturation analysis revealed NAPs to be the most stable amongst the three protein samples examined. Interestingly and quite uniquely, at pH 2.5, there was an increase in CD signal for BoNT complex as a function of temperature, which correlated with the NAPs profile, indicating a shielding effect of NAPs on BoNT complex at low pH. Calculation of the weighted mean of the ellipticities at the T_m for thermal unfolding of toxin and NAPs at neutral and acidic pHs showed variation with that of BoNT complex, suggesting structural reorganization in BoNT complex upon the association of NAPs and BoNT. In conclusion, this study reveals the structural behavior of BoNT complex and NAPs with pH changes substantially, which could be quite relevant for BoNT survival under extreme pH conditions *in vivo*.

Keywords

BoNT; NAPs; molar ellipticity; circular dichroism; thermal denaturation

1 Introduction

BoNT serotypes A-H, are 150 kDa proteins produced by the anaerobic bacterium, *Clostridium botulinum.* Each of these neurotoxins causes debilitating neuroparalytic disease botulism, which is caused by blockade of the acetylcholine neurotransmitter from the

[1]To whom correspondence should be addressed: Bal Ram Singh, Professor and Director, Botulinum Research Center, Institute of Advanced Sciences, 78-540 Faunce Corner Mall Road, North Dartmouth, MA, USA, Telephone: 508-992-2042; Fax: 866-709-1689; bsingh@inads.org.

Ethical standards The experiments carried out in the study are in compliance with the current laws of the United States of America

cholinergic nerve endings [1]. Clinically, botulism is classified into five major types namely, food-borne botulism, infant botulism, wound botulism, hidden botulism and inadvertent botulism [2]. Of these, the food-borne type is the primary form of botulinum intoxication. Upon ingestion through contaminated food, the toxin passes through the GI tract and enters the general circulation to reach the neuromuscular junction, where it exerts its neuroparalytic effects [2,3]. The toxin has a mouse LD dose of 1ng/kg through oral route and it is considered as the most poisonous substance known to man [4]. Owing to its acute toxicity and ease of dissemination, BoNT has been used as a biothreat weapon, further complicating the issues associated with disease spread and control [5].

Structurally, BoNT is produced by the bacterium in the form of a complex with a group of neurotoxin associated proteins or NAPs [6]. Depending on the composition of the complex, it is designated either as M, L or LL form of molecular weights 300 kDa, 500 kDa and 900 kDa, respectively [7]. It has been known from numerous studies that the association of toxin with NAPs confers structural stability to toxin to resist the harsh pH conditions of the GI tract [6,7]. In another related study by Sugii *et al* the oral toxicity of the progenitor toxin was determined to be more than that of the purified toxin and even among the different forms of complex, the combination of L and LL complexes was orally more potent than the M form [6,8].

Upon ingestion, BoNT complex encounters low pH and proteolytic conditions of the GI tract. It is well known that NAPs protect toxin in these adverse conditions and also assist in its translocation across the epithelial layer of the intestinal mucosa [9,10]. The mechanism of this step is not understood at all and this being the only known example where a group of proteins protect another protein against the harsh GI tract conditions, it is therefore of great importance to understand the mechanism of toxin shielding by NAPs. An obvious first step is to examine the response of NAPs to low pH exposure in the stomach and its recovery to neutral pH in the intestinal tract. A recent structure of BoNT/A complex from reconstruction of x-ray and electron microscopy data suggests certain groups within the complex, which might respond to low pH [11], but direct structural data of changes in NAPs with relevant pH conditions is currently lacking. A preliminary work on structural changes in BoNT/A complex and NAPs at pH 3.0 suggested some structural changes but experiments imitating the GI tract pH conditions were not fully carried out [12].

In this study, we compared the secondary structural characteristics of purified BoNT/A toxin, BoNT/A complex and NAPs under both acidic and neutral pH conditions. Also, we monitored the structural changes in the proteins while transitioning them from pH 2.5 to pH 7.2 and assessed the protein's structural flexibility and stability with the changing pH conditions encountered by BoNT during its natural ingestion and trafficking. Our results suggest that structural stability of BoNT/A complex stems from the structural responses of NAPs to low pH and there is a significant adjustment in the structure of BoNT/A and NAPs upon their complex formation.

2 Materials and Methods

2.1 Protein Isolation and Purification

BoNT/A toxin and Type L (500 kDa) BoNT/A complex were isolated from *Clostridium botulinum* type A (Hall strain) according to the bacterial growth conditions and the protein purification protocols adopted by Das Gupta and Sathyamoorthy [13]. The L complex was used for this study as it is the form involved in food poisoning cases. All the other laboratory reagents were purchased from Fisher Scientific (Pittsburgh, PA) and Sigma Chemical Co. (St. Louis, MO).

2.2 Circular Dichroism Spectroscopy

Purified BoNT/A, BoNT/A complex and NAPs were dialyzed in respective pH buffers-10 mM sodium phosphate buffer and 50 mM NaCl, pH 7.2 and 10mM citrate-phosphate buffer with 50 mM NaCl, pH 2.5. For the transition pH conditions, the same protein was dialyzed in acidic pH followed by dialysis in neutral pH and the protein concentration was measured by bicinchoninic acid (BCA) protein assay kit (Thermofisher Scientific, PA). CD data were collected using JASCO J-715 spectropolarimeter (Jasco Inc., MD) equipped with a Peltier temperature control. Far-UV CD spectra in the 190–250nm wavelength region were recorded in a 1.0 mm pathlength cuvette at 25°C for a total of three scans at a scan speed of 20nm/min and with a response time of 8s. The protein concentration used was 0.08–0.1 mg/mL. The percentage of secondary structural elements was calculated using the method of Yang *et al* [14]. For the thermal denaturation analysis, the CD signal at 222 nm was measured in the temperature range of 25–90°C with a heating rate of 2°C/min. The weighted mean of the mean residue ellipticities for thermal unfolding of two proteins was calculated using the formula $((A*\theta_1) + (B*\theta_2))/ (A+B)$, where A and B are the number of amino acid residues in the individual proteins and θ_1 and θ_2 are the mean residue ellipticities at the melting temperature (T_m) for the respective proteins. The thermodynamic parameters of protein unfolding were calculated using the Van't Hoff equation [15].

3 Results

3.1 Secondary structural analysis of BoNT/A proteins

3.1.1 BoNT/A holotoxin—The far UV-CD spectra of BoNT/A showed a similar pattern at pH 7.2 and 2.5 with a double negative maxima at 208 nm and 222 nm, characteristic of an α-helix [16]. The molar ellipticity value was $-2.8*10^4 deg.cm^2/dmol$. The % of secondary structural elements at these two pHs was $18.6 \pm 0.8\%$ α-helix, $42.0 \pm 6.6\%$ β- sheet, $18.3 \pm 3.0\%$ β- turn and $21.2 \pm 2.7\%$ random coil at pH 7.2 and $18.4 \pm 2.6\%$ α-helix, $37.9 \pm 2.7\%$ β-sheet, $20.1 \pm 1.2\%$ β- turn and $23.5 \pm 1.2\%$ random coil at pH 2.5 (Fig. 1a). The transition of the protein from pH 2.5 to 7.2 however resulted in protein precipitation. The precipitates were removed by centrifugation and only clear samples were used for data recording and analysis. The calculation of secondary structural content showed a marked decrease in the % of β-sheet and an increase in random coil structures to 34% at pH 2.5 to 7.2 (compared to 21% at pH 7.2). The percentages of α-helix, β-sheet and β-turn were $29.8 \pm 4.1\%$, $3.8 \pm 0.4\%$ and $32.7 \pm 0.2\%$, respectively (Table 1).

The thermal unfolding curves of BoNT/A showed a distinct denaturation pattern at different pH conditions as shown in Fig. 2a. At pH 7.2, an S-shaped denaturation pattern was observed with a T_m of 54.6 °C. The reversal of pH from 2.5 to 7.2 showed a denaturation pattern similar to that of the pH 7.2 condition. Unlike neutral pH, BoNT/A at pH 2.5 did not exhibit a denaturation pattern even up to the 90°C. Further, estimation of the thermodynamic parameters from the denaturation curves yielded enthalpy and entropy values of 587.0 ± 36.6 kJ/mole and 1782.9 ± 112.2 J/mole.K, respectively at pH 7.2. The free energy change associated with thermal denaturation at 7.2 was 57.9 ± 3.2 kJ/mole. The H, S and G values at pH 2.5 to 7.2 were found to be 823.9 kJ/mole, 2508.9 J/mole.K and 76.3 kJ/mole, respectively (Table 2).

3.1.2 BoNT/A complex—The secondary structural characteristics of BoNT/A complex were determined at pHs 7.2, 2.5 and 2.5 to 7.2. At pHs 7.2 and 2.5, the spectra had double negative maxima around 208 nm and 222 nm with a molar ellipticity of -1.1×10^5 deg.cm^2/dmol at 222 nm (Fig. 1b).The secondary structure comprised of $14.0 \pm 1.3\%$ α-helix, $32.4 \pm 0.6\%$ β- sheet, $17.5 \pm 3.4\%$ β- turn and $36.4 \pm 5.6\%$ random coil at pH 7.2 and $17.1 \pm 3.5\%$ α-helix, $35.3 \pm 2.8\%$ β- sheet, $18.0 \pm 0.3\%$ β- turn and $29.6 \pm 0.4\%$ random coil at pH 2.5. The transition from pH 2.5 to 7.2 also yielded a similar CD signal like the neutral pH with a molar ellipticity of -1.0×10^5 deg.cm^2/dmol. The percentages of α-helix, β- sheet, β- turn and random coil are listed in Table 1.

The thermal denaturation scan carried out for BoNT/A complex at different pHs is shown in Fig. 2b. BoNT complex shared a similar denaturation pattern with that of toxin at pH 7.2 with a decrease in ellipticity as a function of temperature. However, the melting temperature for thermal unfolding of complex was very high at 74.2°C. Surprisingly, in the case of pH 2.5, a unique denaturation pattern was observed with a steep increase in the CD signal with temperature until it stabilized around 82°C with the T_m of 71.1°C. The denaturation pattern with the transition from pH 2.5 to 7.2 was similar to pH 7.2 and had the same T_m value. The H, S and G associated with pHs 7.2, 2.5 and 2.5 to 7.2 was found to be 348.3 ± 40.4 kJ/mol, 1005.7 ± 117.2 J/mol.K and 48.6 ± 5.4 kJ/mol, 532.8 ± 5.2 kJ/mol, 1552.0 ± 15.4 J/mol.K and 70.1 ± 0.6 kJ/mol and 271.2 ± 54.6 kJ/mol, 782.3 ± 157.6 J/mol.K and 38.1 ± 7.6 kJ/mol, respectively (Table 2).

3.1.3 NAPs complex—The secondary structural characteristics of NAPs were examined to understand its toxin protection roles at low pH. The secondary structural predictions revealed that NAPs is predominantly a β-sheet protein. At pH 7.2, % of β-sheet was $61.5 \pm 3.5\%$, whereas the α-helical, β- turn and random coil contents were $7.2 \pm 1.9\%$, $6.9 \pm 0.1\%$, and $24.6 \pm 2.5\%$, respectively. When the pH was lowered to 2.5, there was a decrease in the % of β-sheet to $51.7 \pm 1.9\%$ and an increase in random coil to $30.1 \pm 1.7\%$. At the transition pH 2.5 to 7.2, there was $7.2 \pm 1.3\%$ α-helix, $58.0 \pm 12.3\%$ β-sheet, $7.9 \pm 6.2\%$ β-turn and $26.6 \pm 5.0\%$ random coil, similar to that of pH 7.2 (Table 1). NAPs showed the maximum CD signal at pH 2.5 with the ellipticity of -8.0×10^4 deg.cm^2/dmol, while the values were -6.0×10^4 deg.cm^2/dmol and -4.0×10^4 deg.cm^2/dmol, at the neutral and transition pHs. The ellipticity decreased by 27% and 48% at neutral pH and the transition pH of 2.5 to 7.2, respectively from that of pH 2.5 (Fig. 1c).

Thermal melts at 222 nm revealed that NAPs had the highest thermal stability among the three proteins under study. At pHs 7.2 and 2.5 to 7.2, thermal unfolding patterns of NAPs were similar (S-shaped) to the temperature profiles of toxin and complex with the T_m around 78.8°C. At pH 2.5, the trend of increase in ellipticity with temperature was a notable feature like BoNT/A complex with a T_m at 73.4°C (Fig. 2c). The remarkably high thermal stability of NAPs shows that NAPs possess exceptional structural robustness that protect BoNT complex from thermal denaturation. Estimation of the thermodynamic parameters from the thermal denaturation analysis yielded results similar to that of BoNT/A complex. The values of enthalpy, entropy and Gibb's free energy were higher at pH 2.5 than at pH 7.2 and found to be 506.5 ± 53.7 kJ/mol, 1468.8 ± 156.4 J/mol.K and 68.8 ± 7.1 kJ/mol and 378.8 ± 9.1 kJ/mol, 993.7 ± 89.4 J/mol.K and 82.7 ± 35.8 kJ/mol at pH 2.5 and pH 7.2, respectively. For the protein transition from pH 2.5 to 7.2, the values of ΔH, ΔS and ΔG were 313.3 ± 15.2 kJ/mol, 922.2 ± 74.7 J/mol.K and 38.5 ± 7.1 kJ/mol, respectively, coinciding with the values obtained at pH 7.2 (Table 2).

4 Discussion

The effect of pH on the structure of BoNT proteins is critical for understanding the mechanism of its action at the GI tract level in oral intoxication by BoNT. Physiologically, NAPs protect the toxin during its passage at the low pH conditions and protease-rich environment of the GI tract [7]. To understand the toxin shielding effect of NAPs from structural perspective, the secondary structural characteristics of NAPs, toxin and BoNT complex were compared. While toxin and complex did not show differences in ellipticity between neutral and acidic pHs, the ellipticity in NAPs changed maximally upon exposure to low pH (Fig. 1c). The ellipticity at 222 nm at acidic pH was 1.3 fold more than neutral pH. (Molar ellipticity was $-7.57 \pm 0.06 \times 10^4$ deg.cm^2/dmol at pH 2.5 and $-5.91 \pm 0.03 \times 10^4$ deg.cm^2/dmol at pH 7.2). However, comparing the three proteins at low pH, BoNT complex showed the maximum ellipticity value of $-9.5 \times 10^4 \pm 0.15$ deg.cm^2/dmol at 222 nm, indicating that the protein gains more structure at low pH, a condition that is relevant for its survival in the low pH of the GI tract.

In emulating the physiologically different pH environments encountered by BoNT, the BoNT proteins were exposed to transition pH conditions and their structural stability and flexibility with varying pH were assessed. Toxin and complex exhibited a similar structural pattern at the transition pH 2.5 to 7.2 like pH 7.2 with not much difference in the molar ellipticity value at 222 nm. In the case of NAPs, transition of the protein from pH 2.5 to 7.2 buffer condition resulted in lowering of ellipticity by 46% from that of the acidic pH. An earlier report by Fu *et al* [17] showed that a part of HA-33 could be isolated from BoNT complex at pH 5.5. The recent finding by Gu *et al* reveals that the NTNH part of the NAPs is directly involved in interacting with the toxin and protecting it from the hostile pH environment of the GI tract. They demonstrated the pH-dependent association of the toxin and NTNH where the pH sensing residues Glu^{982} Asp^{1037} in the H_C portion of toxin are protonated at pH 6.0 which stabilizes the association between NBP and BoNT at low pH. On transition from acidic to neutral pH or alkaline pH, the titration of these amino acid groups causes deprotonation of the acidic residues resulting in dissociation of NBP from BoNT [11]. Based on these results and on further research, the exact molecular composition and a

schematic model for BoNT/A complex was proposed showing the direct interaction of toxin with NTNH and HA-33 [21]. These observations indicate pH-dependent structural rearrangements in NAPs, which might be the reason for changes in secondary structure observed with protein exposure from pH 2.5 to 7.2. Another important observation is that both toxin and NAPs showed protein aggregation with pH 2.5 to 7.2 transition but as BoNT complex, they did not show any visible protein precipitation and also yielded higher CD signal compared to NAPs and toxin. This clearly indicates the structural compactness and stability of BoNT complex with pH changes. Thus, examining the structural characteristics at the transition pH unraveled the structural dissimilarities in these proteins, which were otherwise not observed at the individual pHs 7.2 and 2.5.

The structural stability of BoNT proteins at low pH conditions was clearly evident in the thermal unfolding studies. In stark contrast to neutral pH where an S-shaped denaturation pattern was observed, the lack of a denaturation pattern at pH 2.5 for toxin indicates that acidic pH induces structural stability in the protein, thus conferring resistance to thermal denaturation. One of the important findings of this study is the exceptional thermal unfolding behavior of BoNT complex and NAPs at low pH. Unlike the S-shaped denaturation pattern observed at neutral pH, at low pH there was an increase in ellipticity with temperature, which coincided with the NAPs profile. This unique thermal denaturation behavior of NAPs and BoNT complex at low pH clearly indicates that NAPs undergo some molecular reorganization, rendering them structurally robust to protect BoNT complex from thermal denaturation. These observations strongly suggest NAPs stabilizing effect on the structure of BoNT complex under low pH conditions. In fact, to our knowledge, this is the first report demonstrating the unique thermal unfolding behavior of BoNT complex and NAPs at low pH where the CD signal increased as a function of temperature and showed an inverted S-shaped denaturation pattern (Figs. 2b & 2c). The enhancement in CD signal strongly indicates that there is structural refolding in the protein. Hence, low pH triggers conformational changes imparting more secondary structure to NAPs that protect toxin complex from denaturation in the acidic milieu of the stomach. However, the findings by the group of Brandau *et al* were different in the thermal denaturation profile of NAPs, which did not show any increase in ellipticity at low pH and BoNT complex though showed an initial increase in ellipticity at low pH, it eventually decreased above 71°C. We attribute these structural differences to the growth conditions and the protein isolation techniques involved [18,19]. Although their reducing SDS-PAGE results show 7 bands for NAPs, it is still unclear what the molecular composition is. NAPs purified in our lab is passed through a G-100 Sephadex column before eluting it through an anion exchange column to remove the additional impurities and also its exact molecular composition has been determined [20]. Also, there is variation in the buffer and salt composition used for CD analysis in our experiments. It is likely that the differential protein isolation methods and experimental conditions used might be contributing to the differences in the CD thermal denaturation of BoNT complex and NAPs. Nevertheless, their overall observation from the temperature-pH phase diagram indicates that NAPs protect the toxin from denaturation in acidic pH, which is physiologically significant for the survival of toxin in the low pH environment of stomach [12]. Thus, the shielding effect of NAPs on toxin is one of the finest examples of how

accessory proteins assist a protein in overcoming the physiological barriers to exert its function.

Given the toxin protection effects by NAPs at low pH, it is important to understand which of the NAPs proteins is precisely involved in low pH stability of toxin since earlier reports suggest the direct interaction of toxin with both the NTNH and Hn-33 components of NAPs. As explained before, the findings by Gu *et al* strongly suggest that the NTNH part of the NAPs is directly involved in toxin protection in the low pH environment by protonation of the acidic residues of the toxin, which stabilizes the interaction between NTNH and BoNT at low pH [11]. To account for the functional roles of Hn-33 in toxin protection, the work by Sharma *et al* convincingly shows that the toxin was prone to proteolytic degradation by trypsin but in the presence of HA-33, it was more resistant to trypsin action [21]. It was also demonstrated that the mechanism of toxin protection by HA-33 could be either due to the structural changes in the toxin by direct association with HA-33 or by potential blocking of the proteolytic cleavage sites on the toxin by HA-33, which renders the toxin protease-resistant in the GI tract. In effect, the stability of the toxin at acidic pH conditions of the stomach could be attributed to the protective action by NTNH, while HA-33 could be majorly involved in the proteolytic stability of toxin in the protease rich environment of the GI tract. Thus, from the perspective of toxin survival in low pH conditions, it is highly likely that NTNH is the key player in shielding the toxin at low pH. In such a case, the pH stability of the complex would be fairly similar and independent of the type of BoNT complex under study. However, the activity of purified toxin and complex at pH 2.5 was not checked since pH 7.2 is the physiologically significant condition for determination of the protein's endopeptidase activity.

The secondary structural analysis and thermal denaturation curves also shed light on the contributions of NAPs and toxin to the structural make-up of BoNT complex. The greater structural stability of BoNT complex than toxin was evident from the lack of protein aggregation of complex when exposed to transition pH conditions and also higher thermal stability of BoNT complex and NAPs than toxin. This demonstrates a stabilizing interaction between NAPs and toxin in maintaining the structural integrity of BoNT complex in different pH environments. In this regard, the observations by Sharma and Singh showed that HA-33, one of the major NAPs component, interacts directly with toxin and confers proteolytic resistance at acidic and neutral pHs [21]. Also, at a functional level, Cai *et al* had shown that BoNT complex showed a 66% enhancement in the endopeptidase activity compared to purified BoNT which is likely due to the favorable association between NAPs and BoNT [22]. On the other hand, the thermal unfolding nature of these proteins revealed that there was a 29.4% difference in the mean residue ellipticity between BoNT complex and toxin-NAPs combination at their T_m in the transition pH 2.5 to 7.2. The weighted average of the mean residue ellipticity at the T_m for toxin and NAPs unfolding at pH 2.5 to 7.2 was -10.87 ± 0.10 deg.cm^2/dmol, while for BoNT complex, it was calculated as -15.4 ± 0.92 deg.cm^2/dmol. Also, there were differences in the T_m in the thermal denaturation profiles of NAPs and BoNT complex, albeit similarity in their denaturation patterns. Overall, these observations indicate that in addition to the favorable interactions between

NAPs and toxin, BoNT complex further undergoes conformational changes upon the association of toxin and NAPs to ensure structural stability in the protein complex.

In the context of pH effect on the toxic infection process of BoNT, successful intoxication is established when the toxin is able to survive in the dissimilar pH environment of the GI tract- acidic conditions of the stomach and the alkaline intestinal milieu. From the work of Simpson *et al* it is known that NAPs associate with the toxin at low pH and dissociate at pH values above 8.0 [23], which ruled out the possibility to study the structure of BoNT complex in the alkaline pH conditions. Nevertheless, the low pH and thermal unfolding studies demonstrate that the auxiliary proteins play crucial protective roles for the toxin in the GI tract to present the toxin in an active form in the cholinergic nerve terminals.

The BoNT/A complex used in this study is an L (500 kDa) complex. The NAP preparation has 3 HAs and the non-toxin non-hemagglutinin (NTNH). Earlier studies and also the recent work by Gu *et al* reveals that the NTNH part of the NAPs is directly involved in interacting with the toxin and protecting it from the hostile pH environment of the GI tract. They demonstrated a pH-dependent association of the toxin and NTNH where the pH sensing residues Glu^{982} Asp^{1037} in the H_C portion of toxin are protonated at pH 6.0, thus stabilizing the association between NBP and BoNT, thus rendering the toxin stable at low pH conditions [11]. To determine the functional roles of HA-33 in BoNT intoxication, earlier research from our group by Sharma *et al* showed that the toxin was more prone to proteolytic degradation by trypsin but in the presence of HA-33, the toxin complex became more resistant to the trypsin protease activity [21]. It was demonstrated that the mechanism of toxin protection by HA-33 could be either due to the structural changes in the toxin by direct association with HA-33 or by potential blocking of the proteolytic cleavage sites on the toxin by HA-33, which renders the toxin protease-resistant in the GI tract. Based on these results and on further research, the exact molecular composition and a schematic model for BoNT/A complex was proposed showing the direct interaction of toxin with HA-33 [20]. Thus, the current research findings on the relevant roles of NTNH and Hn-33 in toxin protection strongly suggest that the stability of the toxin at acidic pH conditions of the stomach could be attributed to the protective action by NTNH, while HA-33 could be majorly involved in conferring proteolytic resistance to toxin in the protease-rich environment of the GI tract. Thus, from the perspective of toxin survival in the low pH conditions, it is highly likely that NTNH is the key player in shielding the toxin from low pH effects, while Hn-33 assists in protecting toxin against proteases in the GI tract. However, structural reconstruction of the L complex from electron microscopic images [24] has shown no direct interaction between BoNT and HA-33, implying that at least in the presence of NTNH, HA-33 may not directly interact with BoNT. The possibility of HA-33 interacting with BoNT in the absence of the NTNH and other HAs remains and may be the mechanism by which it protects the BoNT against proteases. The other possible mechanism by which HAs may protect the toxin in GI tract may be by faster translocation of the BoNT across epithelial layer of the mucosa in the presence of HAs.

5 Conclusions

The key finding of this study is the remarkable thermal stability of NAPs and BoNT complex at low pH of 2.5. The increase in ellipticity with temperature under acidic pH condition in these proteins affirms structural rearrangements within the NAPs group that renders the structure of BoNT complex highly resistant to low pH-induced protein aggregation. The pH reversibility study shows that among the three proteins, BoNT complex possessed the highest adaptability to varying pHs, a condition that is physiologically significant for maintaining the structural stability in different pH environments of the GI tract. These observations are highly relevant in the context of BoNT intoxication, which might explain the link between structural stability of BoNT complex and its higher toxicity *in vivo*. In parallel, the structural robustness and thermal resistance of BoNT complex might explain the stability and efficacy of BoNT based therapeutics containing NAPs in their formulation.

Acknowledgements

Abbreviations

BoNT	Botulinum Neurotoxin
CD	Circular Dichroism
GI	gastrointestinal
LD	lethal dose
NAP	Neurotoxin associated proteins
UV	ultra violet

References

1. Cherington M. Clinical spectrum of botulism. Muscle Nerve. 1998; 21:701–710. [PubMed: 9585323]

2. Hatheway CL. Botulism: the present status of the disease. Curr Top Microbiol Immunol. 1995; 195:55–75. [PubMed: 8542759]

3. Gill DM. Bacterial toxins: a table of lethal amounts. Microbiol Rev. 1982; 46:86–94. [PubMed: 6806598]

4. Capek P, Dickerson TJ. Sensing the deadliest toxin: technologies for botulinum neurotoxin detection. Toxins (Basel). 2010; 2:24–53. [PubMed: 22069545]

5. Ohishi I, Sugii S, Sakaguchi G. Oral toxicities of Clostridium botulinum toxins in response to molecular size. Infect Immun. 1977; 16:107–109. [PubMed: 326664]

6. Sakaguchi G. Clostridium botulinum toxins. Pharmacol Ther. 1982; 19:165–194. [PubMed: 6763707]

7. Inoue K, Fujinaga Y, Watanabe T, Ohyama T, Takeshi K, et al. Molecular composition of Clostridium botulinum type A progenitor toxins. Infect Immun. 1996; 64:1589–1594. [PubMed: 8613365]

8. Sugii S, Ohishi I, Sakaguchi G. Correlation between oral toxicity and in vitro stability of Clostridium botulinum type A and B toxins of different molecular sizes. Infect Immun. 1977; 16:910–914. [PubMed: 19355]

9. Fujinaga Y, Inoue K, Watarai S, Sakaguchi Y, Arimitsu H, et al. Molecular characterization of binding subcomponents of Clostridium botulinum type C progenitor toxin for intestinal epithelial cells and erythrocytes. Microbiology. 2004; 150:1529–1538. [PubMed: 15133114]

10. Fujinaga Y, Matsumura T, Jin Y, Takegahara Y, Sugawara Y. A novel function of botulinum toxin-associated proteins: HA proteins disrupt intestinal epithelial barrier to increase toxin absorption. Toxicon. 2009; 54:583–586. [PubMed: 19073205]

11. Gu S, Jin R. Assembly and function of the botulinum neurotoxin progenitor complex. Curr Top Microbiol Immunol. 2013; 364:21–44. [PubMed: 23239347]

12. Brandau DT, Joshi SB, Smalter AM, Kim S, Steadman B, et al. Stability of the Clostridium botulinum type A neurotoxin complex: an empirical phase diagram based approach. Mol Pharm. 2007; 4:571–582. [PubMed: 17552543]

13. DasGupta BR, Sathyamoorthy V. Purification and amino acid composition of type A botulinum neurotoxin. Toxicon. 1984; 22:415–424. [PubMed: 6382680]

14. Yang JT, Wu CS, Martinez HM. Calculation of protein conformation from circular dichroism. Methods Enzymol. 1986; 130:208–269. [PubMed: 3773734]

15. Prell JS, Correra TC, Chang TM, Biles JA, Williams ER. Entropy drives an attached water molecule from the C- to N-terminus on protonated proline. Journal of the American Chemical Society. 2010; 132:14733–14735. [PubMed: 20886878]

16. Kelly SM, Jess TJ, Price NC. How to study proteins by circular dichroism. Biochim Biophys Acta. 2005; 1751:119–139. [PubMed: 16027053]

17. Fu F-N, Sharma S, Singh B. A Protease-Resistant Novel Hemagglutinin Purified from Type A Clostridium botulinum. J Protein Chem. 1998; 17:53. [PubMed: 9491928]

18. Malizio CJ, Goodnough MC, Johnson EA. Purification of Clostridium botulinum type A neurotoxin. Methods Mol Biol. 2000; 145:27–39. [PubMed: 10820714]

19. Sathyamoorthy V, DasGupta BR. Separation, purification, partial characterization and comparison of the heavy and light chains of botulinum neurotoxin types A, B, and E. J Biol Chem. 1985; 260:10461–10466. [PubMed: 4030755]

20. Bryant AM, Davis J, Cai S, Singh BR. Molecular composition and extinction coefficient of native botulinum neurotoxin complex produced by Clostridium botulinum hall A strain. Protein J. 2013; 32:106–117. [PubMed: 23334849]

21. Sharma SK, Singh BR. Hemagglutinin binding mediated protection of botulinum neurotoxin from proteolysis. J Nat Toxins. 1998; 7:239–253. [PubMed: 9783262]

22. Cai S, Sarkar HK, Singh BR. Enhancement of the endopeptidase activity of botulinum neurotoxin by its associated proteins and dithiothreitol. Biochemistry. 1999; 38:6903–6910. [PubMed: 10346912]

23. Maksymowych AB, Simpson LL. Structural features of the botulinum neurotoxin molecule that govern binding and transcytosis across polarized human intestinal epithelial cells. J Pharmacol Exp Ther. 2004; 310:633–641. [PubMed: 15140915]

24. Lee K, Gu S, Jin L, Le TT, Cheng LW. Structure of a bimodular botulinum neurotoxin complex provides insights into its oral toxicity. PLoS Pathog. 2013; 9:e1003690. [PubMed: 24130488]
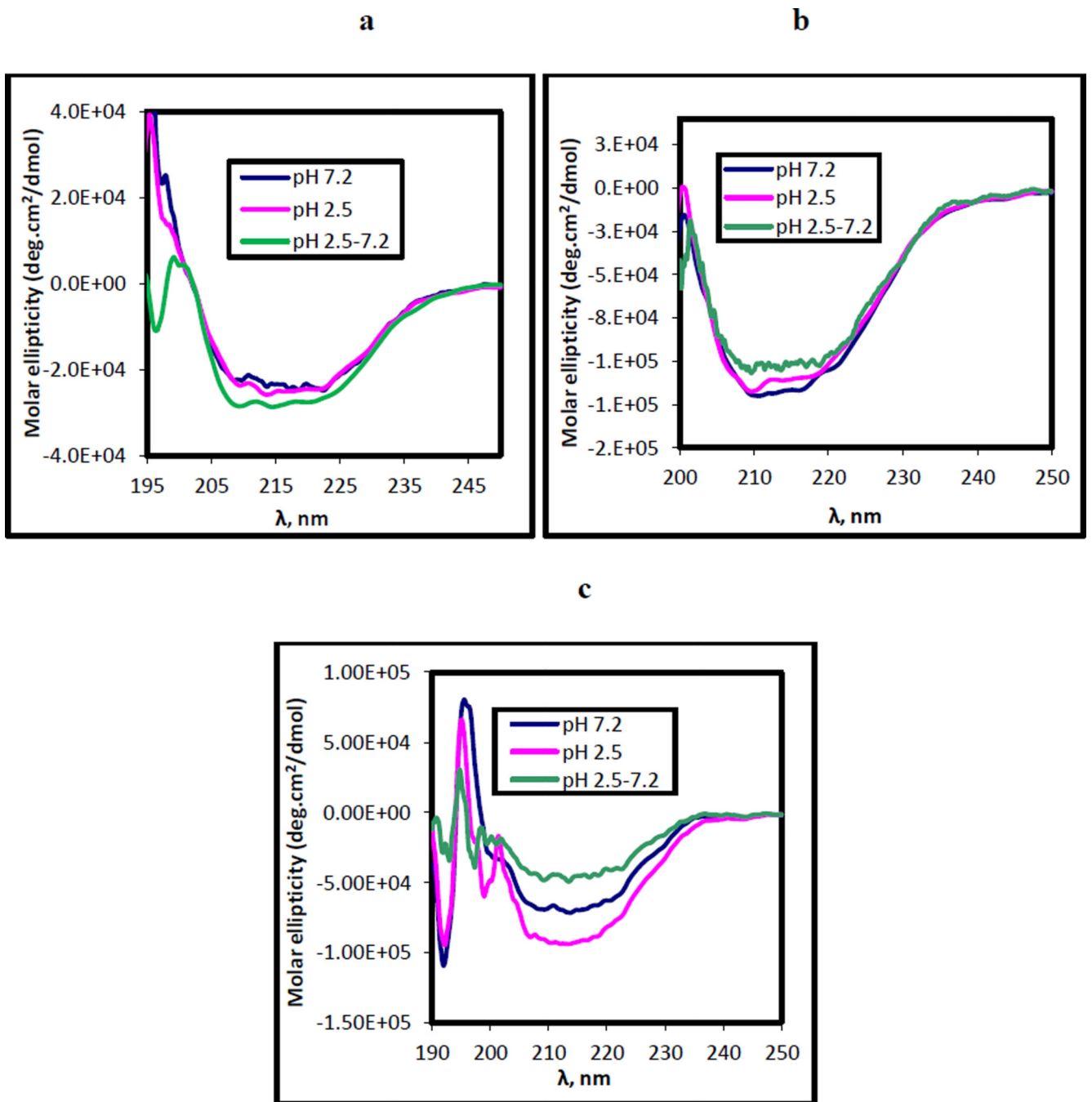
a

b

c

Figure 1.
Far-UV CD spectra of BoNT/A proteins- (a) purified BoNT/A holotoxin (b) BoNT/A complex and (c) NAPs complex at pHs 7.2, 2.5 and 2.5–7.2 at 25° C. 0.08 mg/mL protein in 10 mM sodium phosphate and 50 mM NaCl, pH 7.2 and 10 mM citrate-phosphate buffer and 50 mM NaCl, pH 2.5 were used for the spectral analysis.
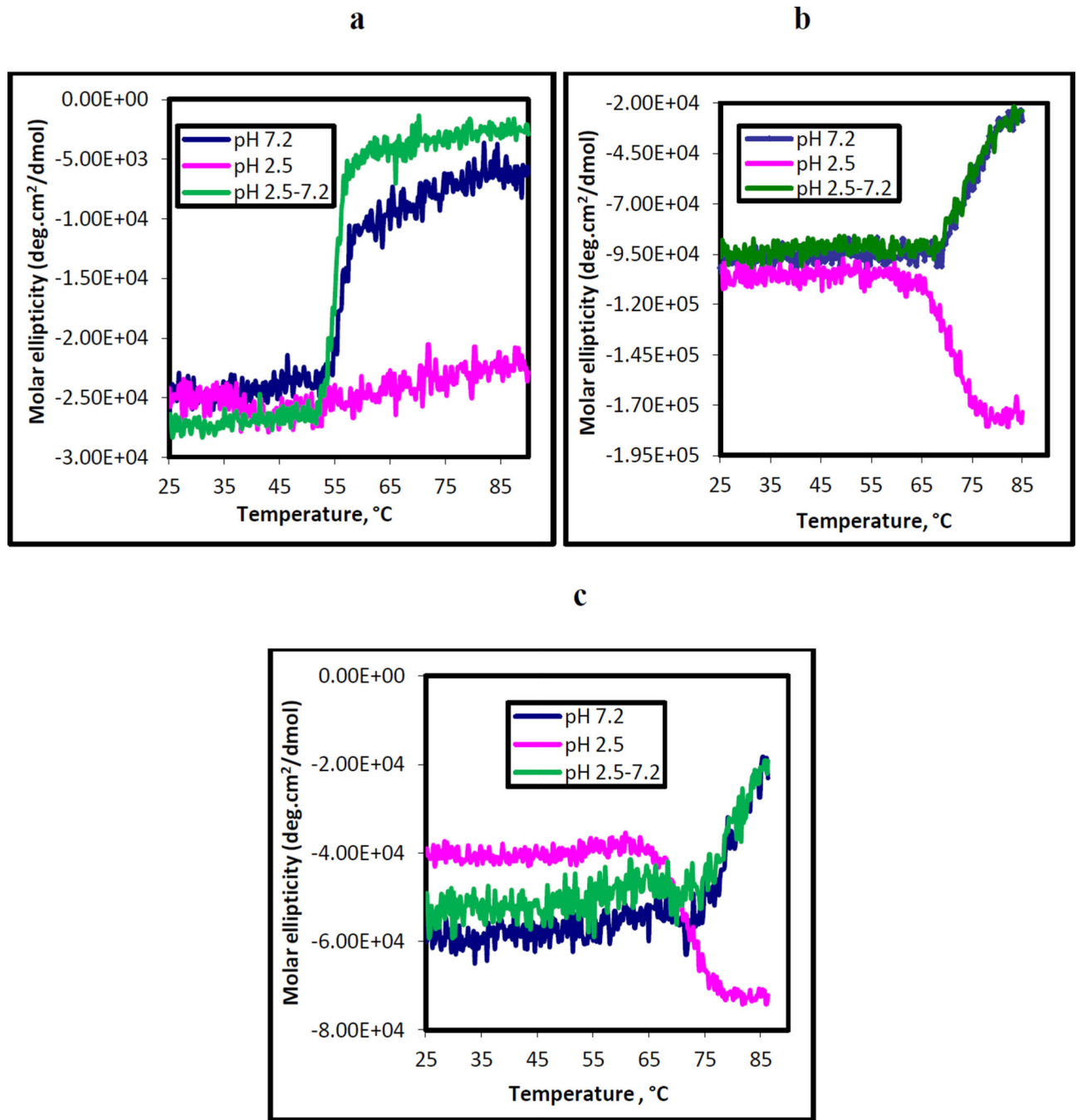
Figure 2.
Thermal unfolding pattern of BoNT/A proteins- (a) purified BoNT/A (b) BoNT/A complex and (c) NAPs complex measured at three different pH conditions by monitoring the ellipticity at 222 nm. The protein buffers used for spectral recordings were 10 mM sodium phosphate and 50 mM NaCl, pH 7.2 and 10 mM citrate-phosphate buffer and 50 mM NaCl, pH 2.5. The spectrum is an average of three spectral scans in the temperature range of 25 °C – 90° C. The rate of heating was 2° C/min and the response time was 8 s.

Table 1

% of secondary structural fractions from the far-UV CD spectra of three BoNT/A protein forms- (a) BoNT/A holotoxin (b) BoNT/A complex and (c) NAPs complex at different pH conditions estimated using the method of Yang *et al.*

pH	(a) BoNT/A holotoxin				(b) BoNT/A complex				(c) NAPs			
	α-helix (%)	β-sheet (%)	β-turn (%)	RC (%)	α-helix (%)	β-sheet (%)	β-turn (%)	RC (%)	α-helix (%)	β-sheet (%)	β-turn (%)	RC (%)
7.2	18.6 ± 0.8	42.0 ± 6.6	18.3 ± 3.0	21.2 ± 2.7	14.0 ± 1.3	32.4 ± 0.6	17.5 ± 3.4	36.4 ± 5.6	7.2 ± 1.9	61.5 ± 3.5	6.9 ± 0.1	24.6 ± 2.5
2.5	18.4 ± 2.6	37.9 ± 2.7	20.1 ± 1.2	23.5 ± 1.2	17.1 ± 3.5	35.3 ± 2.8	18.0 ± 0.3	29.6 ± 0.4	9.1 ± 0.8	51.7 ± 1.9	9.6 ± 1.0	30.1 ± 1.7
2.5–7.2	29.8 ± 4.1	3.8 ± 0.4	32.7 ± 0.2	34 ± 0.3	11.8 ± 0.9	46.9 ± 3.5	13.9 ± 2.8	27.4 ± 0.1	7.2 ± 1.3	58.0 ± 12.3	7.9 ± 6.2	26.6 ± 5.0

Table 2

Estimation of the values of the melting temperature (T_m) and the pseudo thermodynamic parameters- ΔH, ΔS and ΔG from the thermal denaturation profiles of (a) BoNT/A holotoxin (b) BoNT/A complex and (c) NAPs complex using the Van't Hoff equation. The T_m (°C) was measured as the mid-point of the S-shaped portion of the thermal denaturation curve.

pH	(a) BoNT/A holotoxin				(b) BoNT/A complex				(c) NAPs			
	H (kJ/mol)	S (J/mol.K)	G (kJ/mol)	T_m (°C)	H (kJ/mol)	S (J/mol.K)	G (kJ/mol)	T_m (°C)	H (kJ/mol)	S (J/mol.K)	G (kJ/mol)	T_m (°C)
7.2	587.0 ± 36.6	1782.9 ± 112.2	57.9 ± 3.2	54.6 ± 0.2	348.3 ± 40.4	1005.7 ± 117.2	48.6 ± 5.4	74.2 ± 0.2	378.8 ± 9.1	993.7 ± 89.4	82.7 ± 35.8	78.8 ± 0.3
2.5	-	-	-	-	532.8 ± 5.2	1552.0 ± 15.4	70.1 ± 0.6	71.1 ± 0.3	506.5 ± 53.7	1468.8 ± 156.4	68.8 ± 7.1	73.4 ± 0.2
2.5–7.2	823.9	2508.9	76.3	55.0 ± 0.2	271.2 ± 54.6	782.3 ± 157.6	38.1 ± 7.6	74.2 ± 0.2	313.3 ± 15.2	922.2 ± 74.7	38.5 ± 7.1	78.8 ± 0.3